Structure−Function Relationships in Sorcin, a Member of the Penta EF-Hand Family. Interaction of Sorcin Fragments with the Ryanodine Receptor and an *Escherichia coli* Model System†

Carlotta Zamparelli, Andrea Ilari, Daniela Verzili, Laura Giangiacomo, Gianni Colotti, Stefano Pascarella, and Emilia Chiancone*

CNR Center of Molecular Biology, Department of Biochemical Sciences "A. Rossi Fanelli", University of Rome "La Sapienza", 00185 Rome, Italy

Received July 19, 1999; Revised Manuscript Received October 12, 1999

ABSTRACT: Sorcin, a 21.6 kDa cytosolic EF-hand protein which undergoes a Ca^{2+}-induced translocation from cytoplasm to membranes, has been assigned to the newly defined penta EF-hand family. A molecular model of the C-terminal Ca^{2+}-binding domain has been generated using as a template the X-ray coordinates of the corresponding domain in the calpain light subunit, the family prototype [Lin, G., et al. (1997) *Nat. Struct. Biol. 4*, 539−546]. The model indicates that in sorcin the three-dimensional structure is conserved and in particular that of EF1, the novel EF-hand motif characteristic of the family. On this basis, two stable fragments have been obtained and characterized. Just like the native protein, the sorcin Ca^{2+}-binding domain (residues 33−198) is largely dimeric, interacts with the ryanodine receptor at physiological calcium concentrations, and undergoes a reversible, Ca^{2+}-dependent translocation from cytosol to target proteins on *Escherichia coli* membranes. In contrast, the 90−198 fragment (residues 90−198), which lacks EF1 and EF2, does not bind Ca^{2+} with high affinity and is unable to translocate. Binding of calcium to the EF1−EF2 pair is therefore required for the activation of sorcin which uses the C-terminal calcium-binding domain for interaction with the ryanodine receptor, a physiological target in muscle cells.

Sorcin is a 21.6 kDa calcium-binding protein expressed in numerous normal tissues such as heart, muscle, brain, liver, kidney, and adrenal medulla, but identified initially in the cytosol of multidrug resistant cells (hence, the name **so**luble **r**esistance-related **c**alcium-binding prote**in**), where it is overexpressed in conjunction with the drug transporter P-glycoprotein (*1*, *2*). The function of sorcin remains speculative both in multidrug resistance, since the abundance of sorcin does not correlate with the degree of resistance (*2*), and in normal tissues, though a role in signal transduction is suggested by an increasing amount of data. The first experimental evidence in this respect was the observation that sorcin translocates from cytosol to membranes upon binding of calcium. Translocation takes place at micromolar calcium concentrations, is reversed when the cation concentration decreases below this threshold by addition of EGTA (*3*, *4*), and entails interaction with specific target proteins. In cardiac and skeletal muscle cells, these have been identified as the ryanodine receptor (*5*, *6*) and the pore-forming α_1 subunit of voltage-dependent L-type calcium channels (*7*), suggesting a role in interchannel communication during the excitation−contraction cycle. In adrenal medulla, sorcin binds to synexin (annexin VII) and complex formation inhibits synexin-mediated calcium-dependent chromaffin granule aggregation (*8*). Interestingly, the reversible translocation from cytosol to membranes induced by physiological calcium concentrations was discovered in the *Escherichia coli* cells where recombinant sorcin is expressed, a feature exploited in the purification of the protein (*3*). Hence, *E. coli* membranes provide a useful model system for assessing the occurrence of the Ca^{2+}-induced molecular rearrangement that underlies the translocation process. This conformational change leads to the exposure of hydrophobic residues as in numerous EF-hand-containing proteins (*4*). A distinct characteristic of sorcin, however, is the linkage of the binding of Ca^{2+} to pH-dependent changes in the state of association (*4*). The Ca^{2+}-free protein is largely dimeric at neutral and slightly acid pH values, whereas the Ca^{2+}-bound protein gives rise at pH 6.0 to soluble tetramers and at pH 7.5 to high-molecular mass aggregates that precipitate in the presence of free calcium. Since precipitation is unaffected by octyl glucoside but is reversed by EGTA, the aggregates are thought to be stabilized by calcium ions bound to negatively charged groups, possibly carboxylates in a cluster of negative charges, as is often the case when calcium ions bridge different subunits and/or macromolecules (*9*).

The first description of the sorcin sequence indicated a two-domain structure, with an N-terminal domain rich in glycine, proline, and tyrosine residues, and a C-terminal calcium-binding domain containing a pair of high-affinity and a pair of very low-affinity EF-hand motifs and two putative cAMP-dependent protein kinase recognition sites (*10*). The significant similarity with the calpain light chain was also noted and, a few years later, that with grancalcin

† This work was supported in part by grants from the "Ministero per l'Università e Ricerca Scientifica e Tecnologica. Progetto Biologia Strutturale" and CNR Target Project "Biotechnology" to E.C.

* Corresponding author.

10.1021/bi991648v CCC: $19.00
Published on Web 01/04/2000

(*11*). Recently, the X-ray crystal structure of the Ca^{2+}-binding domain of the small calpain subunit, dVI, provided new insight into the structure−function relationships (*12*, *13*). It revealed an unsuspected EF-hand motif in the C-terminal domain whose sequence is conserved in sorcin and grancalcin. This sequence similarity led Maki et al. (*14*) to propose a new family of Ca^{2+}-binding proteins, the penta EF-hand family, which includes also the apoptosis-linked gene product ALG-2 and a hypothetical protein from yeast, YG25. Common characteristics of the family are the dimeric structure of the Ca^{2+}-free form and the capacity to translocate to cell membranes upon calcium binding.

The EF-hand motifs are supersecondary helix−loop−helix structural elements characterized by a canonical 12-amino acid loop sequence that exhibits pentagonal bipyramidal coordination of Ca^{2+} (*15*). The five equatorial Ca^{2+} ligands lie close to a plane that includes the calcium ion and are contributed by the side chains of two acidic residues (positions *Y* and −*Z*), the latter providing two ligands, one polar group (Ser/Thr, position *Z*), and one main chain carbonyl oxygen (position −*Y*). The two apical ligands are furnished by the side chain of an acidic group (position *X*) and a water molecule (position −*X*). In the novel EF-hand variant discovered in calpain dVI, the EF1 site, the loop contains only 11 amino acids and lacks the canonical carboxylate side chains at positions *X* and *Y*. The ligand in position *X* is a carbonyl oxygen furnished by an alanine residue, while a water molecule occupies position *Y*. Thus, the coordination pattern of this new variant involves binding of Ca^{2+} with two carbonyl oxygens (*12*, *13*).

In most Ca^{2+}-binding proteins, the basic structural−functional unit is formed by EF-hand pairs, rather than by single sites. An unusual feature of calpain dVI is the way in which structural pairing of the odd EF-hand, EF5, is achieved. EF5 forms part of the dimer interface and pairs up with the corresponding site of the second monomer in the dimer. In calpain dVI crystals, EF5 is empty even at 200 mM calcium, in accordance with a merely structural role in stabilization of the dimeric structure; EF1−EF3 are saturated with calcium when the cation concentration is 1 mM, whereas EF4 is saturated at 20 mM calcium (*12*, *13*). Calpain dVI undergoes a relatively small calcium-dependent conformational change that is confined to the first 60 amino acids and consists of movement of the EF1 site and of the EF1−EF2 linker region closer to EF3 and EF4 (*12*).

With the aim of gaining a deeper understanding of the structure−function relationships in sorcin, two fragments were prepared by limited proteolysis or recombinant DNA techniques and were characterized. The 33−198 fragment (residues 33−198) represents the complete sorcin Ca^{2+}-binding domain (SCBD)[1] and corresponds to calpain dVI, whereas the 90−198 fragment lacks both EF1 and EF2. In parallel, the molecular model of the SCBD was generated using as a template the coordinates of calcium-bound calpain dVI, kindly provided by S. V. L. Narayana. The functionality of the fragments was tested by following the calcium-dependent binding to the ryanodine receptor and/or the translocation process to *E. coli* membranes used as a model system.

The SCBD model conforms to the expectation that within the penta EF-hand family sequence similarity in the Ca^{2+}-binding domain corresponds to similarity in three-dimensional structure. The properties of the fragments indicate that the capacity of sorcin to interact in a Ca^{2+}-dependent manner with target proteins requires binding of calcium to the EF1−EF2 pair and that the binding site for the ryanodine receptor maps to the Ca^{2+}-binding domain.

EXPERIMENTAL PROCEDURES

Molecular Modeling. Homology modeling was performed on a Silicon Graphics O_2 workstation using modules HOMOLOGY and DISCOVER of the commercial software package INSIGHT II (Insight II User Guide, October 1995, Biosym/MSI, San Diego, CA). The 1.9 Å resolution X-ray crystal structure of calcium-bound domain VI of porcine μ-calpain (*13*) was used as a template to create the model for the corresponding 33−198 domain (residues 33−198) of sorcin. The structurally conserved regions (*16*) were determined first, on the basis of the sequence alignment for sorcin and the small calpain subunit of Van der Bliek et al. (*10*), whose sequence numbering has been adopted. Thereafter, the crystallographic coordinates of the structurally conserved regions were extracted and superimposed onto the corresponding sorcin regions using the module HOMOLOGY. During this procedure, the coordinates of each side chain were kept as close as possible to the atomic positions of the template structure. The coordinates for sequence deletions and sequence variable regions were then generated with the algorithm FIND LOOP followed by preliminary model refinement using subroutines SPLICE REPAIR and RELAX, all of the HOMOLOGY module. Side chain conformations were optimized by manual refinement to remove the most severe steric hindrance. The model was further optimized and refined with several cycles of energy minimization performed with the program DISCOVER. Energy minimization was carried out in vacuo using no cross terms, charges on, with a harmonic potential for bond stretching and the dielectric constant set to 1.0. An initial minimization was performed on the monomer model with fixed main chain atoms. A tethering force was applied to side chain atoms with a force constant of 50 kcal/Å^2; 100 iterations of the steepest descent minimizer were carried out, and the total energy decreased from −43737.39 to −44185.87 kcal. Subsequently, the dimer was energy minimized under the same conditions, fixing the main chain atomic positions and restraining the distances between the ligands and Ca^{2+} with a force of 80 kcal mol^{-1} Å^{-1}. The total energy decreased from 9685295.64 to −141744.99 kcal. A final minimization was carried out on the dimer with a tethering force constant of 100 kcal/Å^2 to all atoms of the molecule, Ca^{2+} and ligands constrained as before, ω angles forced to the trans conformation with a force of 200 kcal mol^{-1} Å^{-1}, and 50 iterations of conjugate gradients. The total energy decreased from 16265627.82 to 440.33 kcal. Last, the effects of a solvent shell (8 Å radius) and of a distance-dependent dielectric constant were tested. The system was minimized with conjugate gradients fixing all atoms of the model and leaving

[1] Abbreviations: CD, circular dichroism; EDTA, ethylenediaminetetraacetic acid; EGTA, ethylene glycol bis(β-aminoethyl ether)-*N*,*N*,*N*′,*N*′-tetraacetic acid; FPLC, fast protein liquid chromatography; PVDF, polyvinyl difluoride; SCBD, sorcin calcium-binding domain corresponding to fragment 33−198; Quin 2, 2-({2-[bis(carboxymethyl)-amino]methyl}phenoxy)-6-methoxy[bis(carboxymethyl)amino]quinoline.

water molecules free to move. The system was minimized to a maximum derivative of 0.1 kcal mol^{-1} $Å^{-1}$. The dimer model thus obtained, when superimposed on the initial one, yielded a rms deviation of 0.79 Å on the position of all Cα atoms. Only minor differences were detected in a few side chain χ angles and at the Ca^{2+}-binding sites.

The program PROCHECK (*17*) was employed to assess the stereochemical properties of the model. A three-dimensional profile, which measures the compatibility of a protein model with its sequence, was used to verify the final protein fold (*18*). Secondary structure assignment and surface calculations were carried out with the program HOMOLOGY using the commands SURFACE, which calculates the van der Waals surface, and SECONDARY RENDER MOLECULE, which creates a Richardson style rendering of the protein secondary structure.

Figures have been drawn with MOLSCRIPT (*19*).

Preparation of Sorcin and Sorcin Fragments. Chinese hamster ovary recombinant sorcin was expressed in *E. coli* BL21(DE3) cells, kindly provided by M. B. Meyers, and was purified as previously described (*3*). The protein concentration was determined spectrophotometrically at 280 nm using a molar extinction coefficient of 29 400 (*3*). The 33−198 domain was obtained by limited proteolysis of the native protein with endoproteinase AspN (sequencing grade, Boehringer Mannheim, Mannheim, Germany). The reaction was carried out at 30 °C for 16 h in 100 mM Tris-HCl buffer at pH 7.4 using a 1 mg/mL sorcin solution and an enzyme: substrate ratio of 1:500 (w/w); it was stopped by addition of 10^{-4} M EDTA. One main proteolytic fragment is obtained due to specific cleavage of the peptide bond N-terminal to Asp33 as determined by automatic Edman degradation with a gas-phase Sequenator (model 476 A, Applied Biosystems, Foster City, CA). The 33−198 domain was separated from the undigested protein by anion-exchange chromatography on a Mono Q column, connected to an FPLC apparatus (Pharmacia, Uppsala, Sweden). The digestion mixture was applied to the column after dialysis against 10 mM Tris-HCl buffer at pH 7.5. The column was equilibrated with the same buffer and was eluted with a 0 to 0.5 M NaCl gradient. The 33−198 fragment elutes at 0.15 M NaCl; its concentration was determined spectrophotometrically at 280 nm using a molar extinction coefficient of 22 000 calculated according to Edelhoch (*20*).

For the expression of the 90−198 fragment, the cDNA of the native protein (*10*) was digested with *Nco*I, which cleaves in two sites corresponding to Met1 and Met90. The large DNA fragment that was obtained was ligated by its cohesive ends, while the small fragment was discarded. The final DNA product was inserted into the pET32b(+) vector (which contains an N-terminal histidine tag, a thrombin, and an enterokinase cleavage site) for expression of the 90−198 sorcin fragment as a thioredoxin fusion product (Novagen, Madison, WI). The expression of the fusion protein was performed as described for native sorcin (*3*). The purification of the fragment was carried out according to the Novagen protocol using a nickel nitrilotriacetate affinity chromatography column (Qiagen, Hilden, Germany); its concentration was determined spectrophotometrically at 280 nm using a molar extinction coefficient of 18 000 calculated according to Edelhoch (*20*).

Characterization of Sorcin and Its Fragments. Sedimentation velocity and equilibrium experiments were performed in 0.1 M Tris-HCl (pH 7.5) containing 1 mM EGTA at 10 and 20 °C in a Beckman Optima XL-A ultracentrifuge which was run at 40 000 and 25 000 or 30 000 rpm, respectively. Absorption scans along the centrifugation radius were carried out at a wavelength of 280 nm. Weight average sedimentation coefficients were calculated using the software DCDT for associating systems provided by W. Stafford (Boston Biomedical Research Institute, Boston, MA), and were reduced to $s_{20,w}$ using standard procedures. Sedimentation equilibrium data were edited with REEDIT (J. Lary, National Analytical Ultracentrifuge Center, Storrs, CT) and fit with NONLIN (*21*) to a single species and to a monomer−dimer equilibrium. The partial specific volume of 0.723 mL/g was calculated from the amino acid composition.

Circular dichroism spectra were recorded in the 190−250 nm region using a Jasco J-710 spectropolarimeter. The α-helical content was calculated according to Yang et al. (*22*). The experiments were performed at 25 °C in 10 mM Tris-HCl buffer at pH 7.5.

Fluorescence titrations were carried out in a Fluoromax spectrofluorimeter, in 0.1 M sodium acetate buffer (pH 6.0); excitation was at 280 nm (slit width of 0.5 nm). The emission signal was followed between 300 and 400 nm (slit width of 0.5 nm). The temperature was 25 °C. After each calcium addition, the solution was left to equilibrate for at least 2 min. Indirect titrations were performed in 0.1 M Tris-HCl at pH 7.5 and 25 °C, in the presence of the fluorescent calcium chelator Quin 2, according to Bryant (*23*). The experiments were carried out as described in ref *4*. The excitation wavelength was 339 nm (slit width of 0.5 nm); the increment of emission intensity due to calcium binding to Quin 2 was followed at 492 nm (slit width of 0.5 nm). Control experiments were performed on Quin 2 alone and on native sorcin. At the end of each titration, the fluorescence intensities corresponding to zero Ca^{2+} and excess Ca^{2+} were determined by addition of 5 mM EGTA and 50 mM $CaCl_2$, respectively. The overall binding constant was obtained by fitting the experimental data with a program written with MATLAB (The Math Works, Natick, MA). The degree of saturation of Quin 2 (Y) was calculated from the equation $Y = (I - I_{min})/(I_{max} - I)$, where I is the observed fluorescence intensity and I_{max} and I_{min} are the fluorescence intensities corresponding to zero Ca^{2+} and excess Ca^{2+}, respectively. The concentration of free calcium, x, was calculated using the equation

$$C - \frac{K_3 E_T x}{1 + K_3 x} + \frac{K_1 S_T x + 2K_1 K_2 S_T x^2}{1 + K_1 x + K_1 K_2 x^2} - x = 0$$

where C is the total calcium concentration, E_T is the chelator concentration, S_T is the total concentration of sorcin, K_1 and K_2 are the sorcin calcium binding constants, and K_3 is the Quin 2 calcium binding constant (1.2×10^7 M^{-1}; *22*). The stoichiometry of 2 equiv of Ca^{2+}/sorcin monomer, determined from the absorbance change observed upon mixing Ca^{2+}-saturated Quin 2 and sorcin in stopped-flow esperiments (*4*), was used.

Interaction of Sorcin and Its Fragments with E. coli Membranes. The reversible Ca^{2+}-dependent interaction with

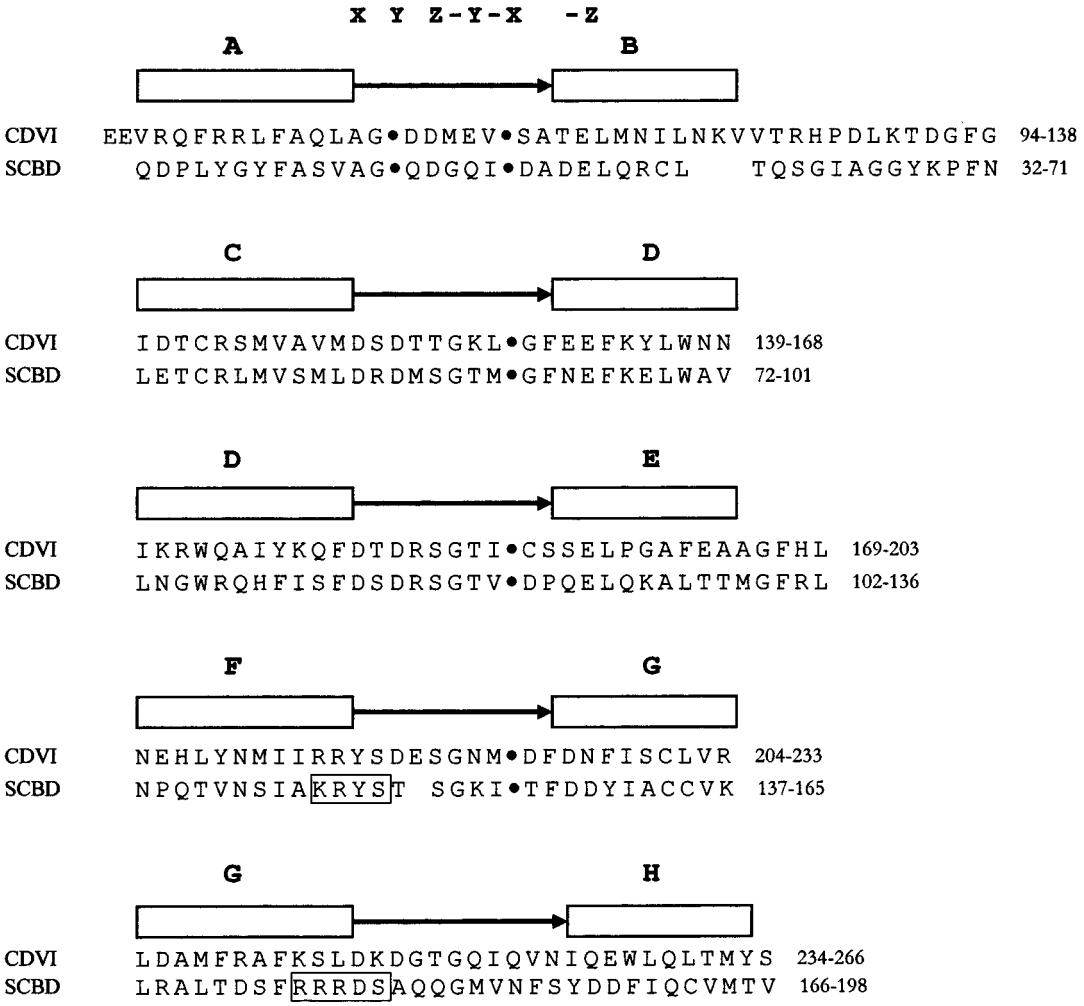

FIGURE 1: Amino acid sequence alignment of the sorcin calcium-binding domain (SCBD) and of calpain dVI (CDVI) according to Van der Bliek et al. (*10*). Helices are represented as rectangles and labeled A−H; the calcium binding loops are denoted by arrows. Residues that form the calcium coordination sphere are labeled *X*, *Y*, *Z*, −*Y*, −*X*, and −*Z*. The solvent molecules that coordinate the calcium ion are denoted by a dot. The two potential cAMP-dependent phosphorylation sites proposed in ref *10* are boxed.

E. coli membranes was tested as described in ref *3* and described in detail in the figure legends.

Interaction of Sorcin and the 33−198 Fragment with the Ryanodine Receptor. Sorcin and the 33−198 fragment were subjected to electrophoresis on a 15% polyacrylamide gel under denaturing conditions (*24*) and transferred to PVDF membranes (Problott, Applied Biosystems) in transfer buffer [25 mM Tris-HCl, 192 mM glycine, and 20% methanol (pH 8.3)] for 1 h at 100 mA (*25*). For Western blot analysis, the PVDF membranes were incubated for 2 h at room temperature in 1% gelatin dissolved in TBS buffer [20 mM Tris-HCl (pH 7.5), 0.5 M NaCl, and 10^{-5} M $CaCl_2$ or 10^{-4} M EGTA] containing 5 γ/mL of terminal cisternae vescicles from rabbit skeletal muscle enriched with the ryanodine receptor, kindly provided by F. Zorzato. Subsequently, the membranes were incubated with the anti-ryanodine receptor monoclonal antibody (INALCO) at a dilution of 1:3000 in 1% gelatin in TBST (TBS containing 0.05% Tween 20). The blots were developed by incubation with alkaline phosphatase conjugate monoclonal anti-mouse IgG (Sigma, St. Louis, MO) in 1% gelatin in TBST. Control experiments ruled out the existence of cross-reactivity between the anti-ryanodine receptor antibody and sorcin.

RESULTS

Three-Dimensional Model of the Sorcin Calcium-Binding Domain (SCBD). The sequence alignment of sorcin and of calpain proposed by Van der Bliek et al. (*10*) shows that the degree of amino acid sequence identity in the Ca^{2+}-binding domain is ≈30% (Figure 1). The overall topology of the SCBD model, which is also shown in Figure 1, confirms the presence of the penta EF-hand motif revealed by the calpain dVI crystal structure (*12*−*14*).

The SCBD three-dimensional model exhibits good stereochemical quality (*17*). The accuracy in comparison with the calpain dVI structure, assessed according to the method of Lüthy et al. (*18*), is likewise good. Thus, the three-dimensional profiles obtained for the two proteins with windows of 11 and 21 residues are very similar and have positive scores, indicative of correctly folded proteins. In sorcin, a negative score is obtained only for the 160−198 region, a finding that is correlated to the presence of several solvent-exposed hydrophobic residues which are buried upon dimer formation (see below) rather than to a misfolded structure.

The general folding pattern of the SCBD closely resembles that of calpain dVI. Only eight α-helical segments are

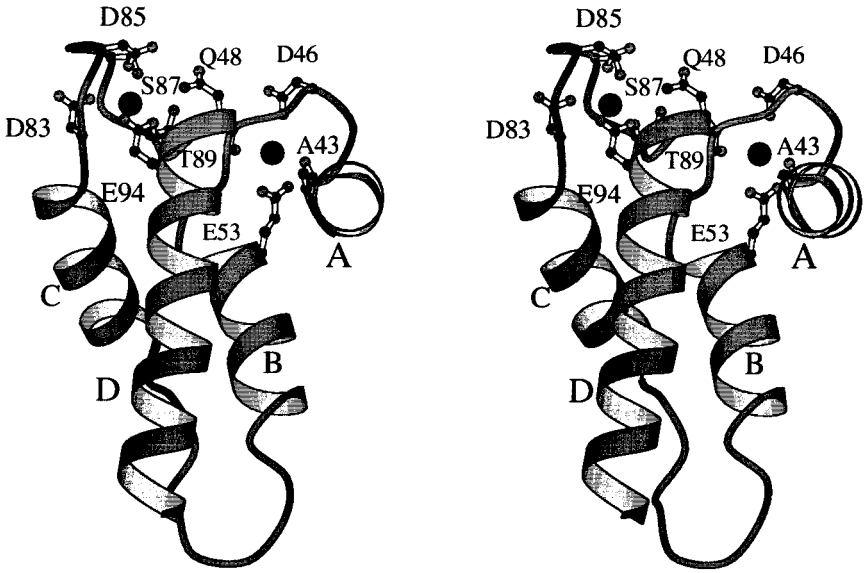

FIGURE 2: Stereoview of the EF1−EF2 pair in the sorcin calcium-binding domain. The EF-hands are both in the open conformation. Helices A−D are labeled, and the residues that form the calcium coordination sphere for each loop are denoted. The calcium ions are represented as spheres. The solvent molecules that coordinate calcium are not shown.

predicted for five EF-hand motifs, since helices D and G contribute residues to two consecutive EF-hands (EF2−EF3 and EF4−EF5, respectively). In sorcin, as in calpain dVI, the novel EF1 calcium-binding site comprises 11 amino acids with substitutions of the canonical carboxylate oxygen of Asp at positions *X* and *Y*. The ligands at these positions are a carbonyl oxygen (contributed by Ala43 in sorcin) and a water molecule. EF1 is connected to EF2 through a loop that interacts with helices B and D, giving rise to a compact EF-hand pair (Figure 2). In sorcin, this loop is shorter than in calpain dVI by three residues; however, this deletion does not necessitate large changes in the conformation of the polypeptide backbone. The EF2 site has a typical coordination with Asp, Asp, and Glu residues at conserved positions *X*, *Y*, and $-Z$. The calcium ligand at position $-Y$ is the carbonyl oxygen of Thr89 in sorcin and of Lys156 in calpain dVI; at position *Z*, the ligand is the oxygen furnished by Ser87 in sorcin and by Thr154 in calpain dVI. However, in the calpain IV domain of the large subunit, this position is occupied by Ser as in sorcin (*14*). Both EF1 and EF2 are in the so-called "open" conformation (*15*, *26*), the interhelical angles being about 120°.

In the second EF-hand pair, the EF3 site has identical Ca^{2+}-binding ligands in sorcin and calpain dVI. EF4 is atypical in terms of the consensus EF-hand sequence and mode of calcium coordination. Thus, in calpain dVI crystals, calcium is bound at the N-terminus of the F helix at a concentration of 200 mM. The apical ligands in sorcin are Thr150 and a water molecule (Asp223 and a water molecule occupy the corresponding positions in calpain dVI). The equatorial ligands in calpain dVI are Asp135 (*Z*) from the loop connecting EF1 and EF2, which is substituted with Lys68 in sorcin, Asp225 ($-Y$), and Asn226 ($-Z$) which correspond to Asp157, Asp158, and a water molecule in sorcin. In EF3 and EF4, the helical arrangement resembles that of the low-affinity, empty Ca^{2+}-binding site of troponin C and hence is in the so-called "closed" conformation (*15*, *26*).

The loop of the fifth, odd EF-hand site has a two-residue insertion in both proteins. Thereby, the conserved Glu residue

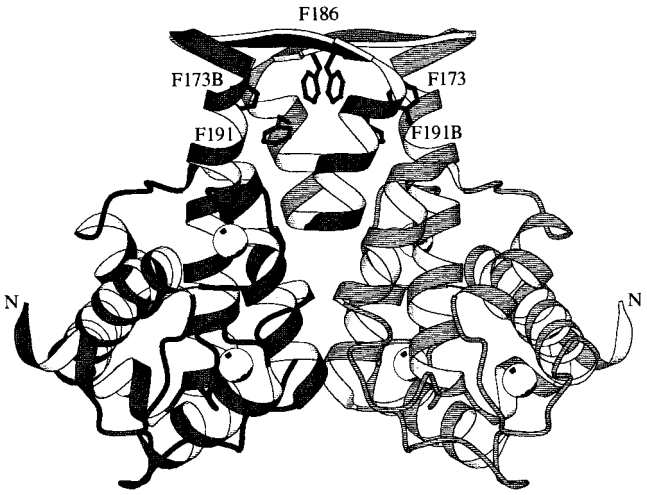

FIGURE 3: Ribbon representation depicting the interaction between monomers in the dimer of the sorcin calcium-binding domain. The phenylalanine residues at the interface are denoted and labeled. The calcium ions are represented as spheres.

at position *Z* is shifted at a distance that is too long for an effective coordination of calcium. In fact, this site is empty in calpain dVI crystals at 200 mM calcium. In sorcin, the calcium affinity is likely to be even lower since the conserved Asp residue at position *Y* is substituted with alanine (Ala179).

The SCBD associates into dimers in solution (see below). The SCBD dimer was modeled assuming the same geometry of the calpain dVI quaternary structure. A 2-fold symmetry axis runs along the four-helix bundle created by the packing together of the EF5 helices, while the loops form an antiparallel two-stranded β-sheet (Figure 3). Several hydrophobic residues in the 160−198 region become buried at the dimer interface, thereby providing a significant degree of stabilization, e.g., Phe186 and Phe191 from the H helices (in calpain dVI, the corresponding residues are Trp259 and Val254).

In the SCBD dimer model, only one of the two potential cAMP-dependent protein kinase phosphorylation sites predicted by the sequence (Figure 1) is exposed to solvent,

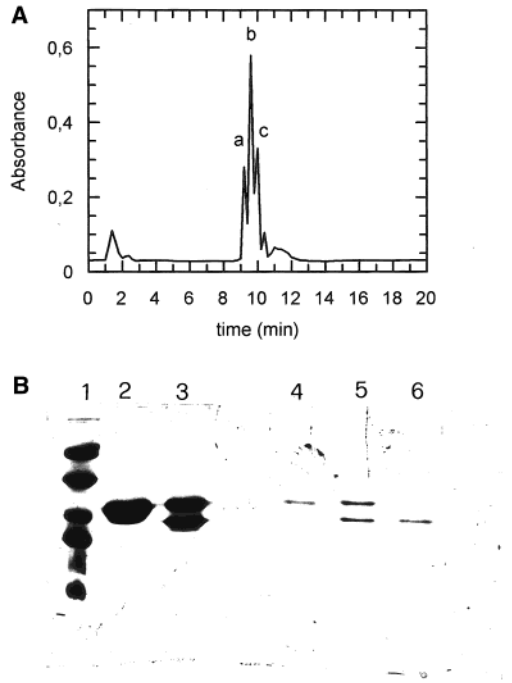

FIGURE 4: Purification of the sorcin calcium-binding domain (SCBD). (A) Elution diagram of a digestion mixture with AspN loaded onto a Mono Q anion exchanger column equilibrated with 10 mM Tris-HCl (pH 7.5). Elution was performed with a 0 to 0.5 M NaCl gradient, which was started 5 min after loading the protein. (B) SDS−polyacrylamide gel electrophoresis pattern of the peaks retained on the Mono Q column: lane 1, molecular mass markers (46, 30, 21.5, 14.3, 6.5, and 3.4 kDa); lane 2, sorcin; lane 3, digestion mixture loaded on the Mono Q column; lane 4, fraction a, containing sorcin; lane 5, fraction b, containing sorcin and the SCBD; and lane 6, fraction c, containing the SCBD. Fractions a−c are in a 1:2:1 ratio, indicating that the SCBD and the sorcin monomer form a statistical hybrid.

namely, Arg174, Arg175, Arg176, Asp177, and Ser178 (RRRDS), since the other site, Lys146, Arg147, Tyr148, and Ser149 (KRYS), is embedded in the dimer interface.

Properties of the Sorcin Calcium-Binding Domain, the 33−198 Fragment. The 33−198 fragment is the principal product obtained by limited proteolysis of sorcin with endoproteinase AspN. Its existence as a stable species demonstrates the similarity in three-dimensional structure of the Ca^{2+}-binding domains within the penta EF-hand family. The elution pattern of the digestion mixture from an anion-exchange chromatography column (Figure 4) reveals that the SCBD forms a statistical hybrid with the undigested protein. In turn, hybridization, which affects adversely the yield of the purified domain, indicates that both sorcin and the SCBD are in a finite association−dissociation equilibrium. This indication was confirmed in sedimentation equilibrium experiments carried out with the native protein over the concentration range of 10−50 μM, which yielded a monomer−dimer association constant of 3×10^5 M^{-1}. In good agreement with these data, a $K_{1,2}$ value of $0.8-1.0 \times 10^5$ M^{-1} can be calculated from the weight average sedimentation coefficients measured over the same concentration range ($s_{20,w}$ = 3.2−3.3 S), assuming a spherical shape (*27*).

The purified SCBD sediments in the ultracentrifuge with a weight average $s_{20,w}$ of 3.1−3.2 S at a concentration of 7−11 μM both in the absence and in the presence of 2 equiv of Ca^{2+}/monomer in the buffer. This value, assuming a hydrodynamic behavior as a sphere (*27*), corresponds to a

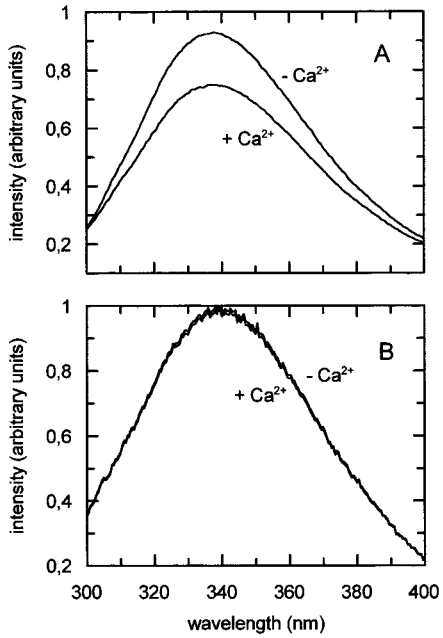

FIGURE 5: Fluorescence emission spectra of sorcin (A) and the SCBD (B) in the absence and presence of calcium. The sorcin concentration was 6.9 μM; the SCBD concentration was 8.3 μM in 100 mM Tris-HCl buffer (pH 7.5), and the calcium concentration was 25 μM.

weight average molecular mass of about 32 kDa and yields an association constant $K_{1,2}$ of about 0.9×10^5 M^{-1}, indicating that the tendency of the SCBD to dimerize is similar to that of the native protein. In turn, this result is consistent with the ability of the SCBD and the native protein to hybridize and with the amount of hybrid formed in the experiment whose results are depicted in Figure 4. The far-UV CD spectrum indicates that the α-helical content (*22*) is unchanged upon addition of calcium and corresponds to about 60%, in very good agreement with the value predicted from the three-dimensional model (62%). The fluorescence emission spectrum is characterized by a maximum at 339 nm, which is red-shifted by 2 nm relative to that of sorcin. The fluorescence intensity is essentially unchanged upon addition of calcium, whereas it is quenched significantly in the native protein (Figure 5); under the conditions that are used (7 μM protein at pH 7.5), precipitation in the presence of excess calcium is negligible.

The calcium affinity was estimated by means of indirect fluorescence titration experiments carried out in 0.1 M Tris-HCl at pH 7.5 in the presence of Quin 2, using native sorcin and Quin 2 as controls. Sorcin and the SCBD compete effectively with Quin 2 for the binding of Ca^{2+} as indicated by the positions of the respective titration curves (Figure 6). The data of native sorcin and of the SCBD can be fitted with the stoichiometry of 2 equiv of Ca^{2+}/monomer and the overall affinity constant (2×10^{12} M^{-2}) determined by Zamparelli et al. (*4*).

The functionality of the SCBD was tested with both the ryanodine receptor and *E. coli* membranes. Western blot experiments show that the SCBD, just like native sorcin, associates with the ryanodine receptor when the buffer contains calcium at physiological concentrations (Figure 7), whereas no association occurs in the presence of EGTA as indicated in control experiments (data not shown). Moreover, the SCBD undergoes a reversible Ca^{2+}-dependent translo-

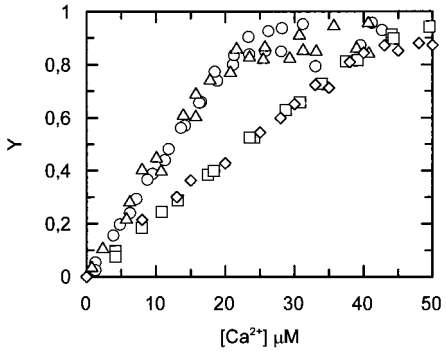

FIGURE 6: Fluorescence titration of sorcin, the SCBD, and the 90−198 fragment with calcium in the presence of Quin 2. The degree of saturation of Quin 2 is plotted as a function of total calcium concentration. Sorcin (□), the SCBD (◇), and the 90−198 fragment (△) at a concentration of 25 μM were titrated with calcium in the presence of 25 μM Quin 2 in 0.1 M Tris-HCl at pH 7.5 and 25 °C. Data from a control titration of Quin 2 alone with calcium (○) are also shown.

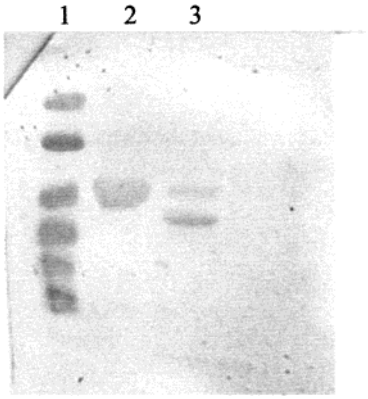

FIGURE 7: Interaction of sorcin and the SCBD with the ryanodine receptor. Sorcin and an AspN digestion mixture containing the SCBD were subjected to SDS−PAGE and transferred to PVDF membranes. The PVDF membranes were incubated with the ryanodine receptor and subsequently with anti-ryanodine receptor monoclonal antibody: lane 1, molecular mass markers (46, 30, 21.5, 14.3, 6.5, and 3.4 kDa); lane 2, sorcin; and lane 3, AspN digestion mixture containing sorcin and the SCBD. For buffer conditions, see Experimental Procedures.

cation to *E. coli* membranes under the same conditions as the native protein (Figure 8). Thus, both the SCBD and sorcin are associated with the membrane fraction of *E. coli* cells when $CaCl_2$ is added to the buffer and are released to the supernatant when that membrane fraction is treated with EGTA.

Properties of the 90−198 Fragment. The solution properties of the 90−198 fragment, characterized by means of circular dichroism and sedimentation velocity experiments, indicate that it retains a native conformation. Thus, the CD spectra in the far-UV region show that the α-helical content is about 55% (*22*), as predicted by the model. The sedimentation coefficient ($s_{20,w} \approx 2.8$ S) indicates that the fragment is largely dimeric, again in full agreement with the exposure to solvent of the missing EF1- and EF2-hand motifs (Figure 3).

As for the SCBD fragment, the calcium affinity was estimated by means of indirect fluorescence titration experiments. The results included in Figure 6 show that the presence of the 90−198 fragment does not affect the titration of Quin 2. Hence, the affinity of this fragment for calcium

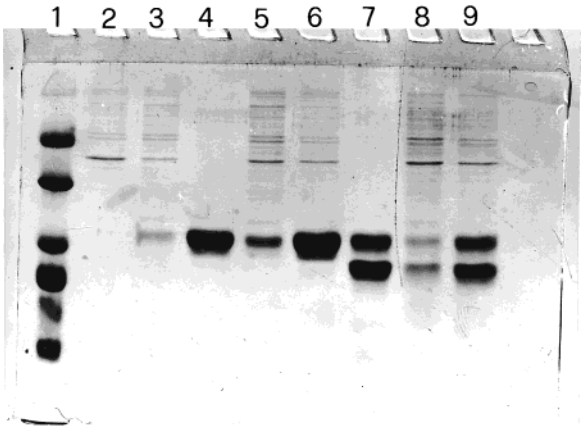

FIGURE 8: Calcium-dependent translocation of sorcin and of the SCBD to *E. coli* membranes assessed by SDS−PAGE. Translocation was promoted by exposing *E. coli* BL21(DE3) membranes for 10 min to the protein under analysis in 100 mM Tris-HCl at pH 7.5 and pCa 5; thereafter, the mixture was centrifuged at 16000*g* for 10 min, and the supernatant was analyzed (s_1). The pellet was used to test the reversibility of the translocation process. It was resuspended in the same buffer containing 2 mM EGTA; the mixture was centrifuged at 16000*g* for 10 min and the supernatant analyzed (s_2): lane 1, molecular mass markers (46, 30, 21.5, 14.3, 6.5, and 3.4 kDa); lanes 2 and 3, s_1 and s_2 obtained with membranes not exposed to sorcin; lane 4, sorcin; lanes 5 and 6, s_1 and s_2 obtained with membranes exposed to sorcin; lane 7, AspN digestion mixture containing sorcin and the SCBD; and lanes 8 and 9, s_1 and s_2 obtained with membranes exposed to the AspN digestion mixture.

must be at least 2 orders of magnitude lower than that of the fluorophore [K_A(Quin 2) = 1.2×10^7 M^{-1}]. It is worth mentioning that when the amount of added calcium exceeds 2 equiv/monomer, the slight precipitation observed with the native protein and the SCBD fragment does not take place. The affinity for calcium could not be assessed in direct fluorescence titration experiments since the intensity of the fluorescence emission spectrum is unchanged after addition of millimolar calcium, as in the case of the SCBD.

The reversible Ca^{2+}-dependent interaction with membranes was tested using the *E. coli* model system (*3*). The 90−198 fragment does not translocate even in the presence of 10 mM $CaCl_2$ (data not shown). The interaction with the ryanodine receptor was not tested given the paucity of available receptor and the results of the titration experiments depicted in Figure 6.

The difference in translocation ability of the 33−198 and 90−198 fragments to the *E. coli* membrane model system implies that the binding of 2 equiv of Ca^{2+} to the EF1−EF2 pair suffices to trigger the functionally relevant conformational change and that calcium in excess over this amount is free and hence able to promote aggregation of sorcin in the absence of membranes (*4*). To further substantiate this contention, the following sedimentation velocity experiment was carried out. A 23.3 μM sorcin solution in 100 mM Chelex-treated Tris-HCl buffer at pH 7.5 was titrated in the ultracentrifuge cells with up to 5 equiv of calcium/monomer. The $s_{20,w}$ value is always 3.2−3.3 S, whereas the absorbance at 280 nm decreases due to formation of sorcin aggregates when the level of calcium exceeds 2 equiv/monomer (Figure 9).

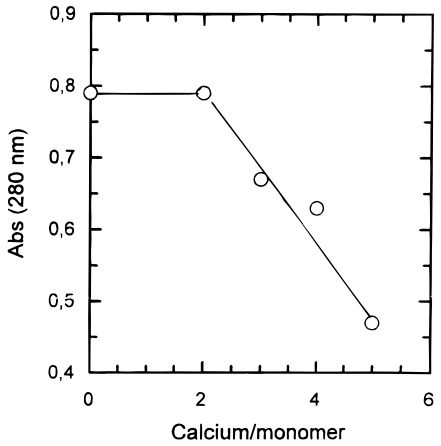

FIGURE 9: Titration of sorcin with calcium in the analytical ultracentrifuge. Different amounts of calcium were added just before the sedimentation velocity experiment to 23 μM sorcin in Chelex-treated 100 mM Tris-HCl buffer at pH 7.5; the absorbance in the plateau region is plotted as a function of the Ca^{2+}:monomer molar ratio.

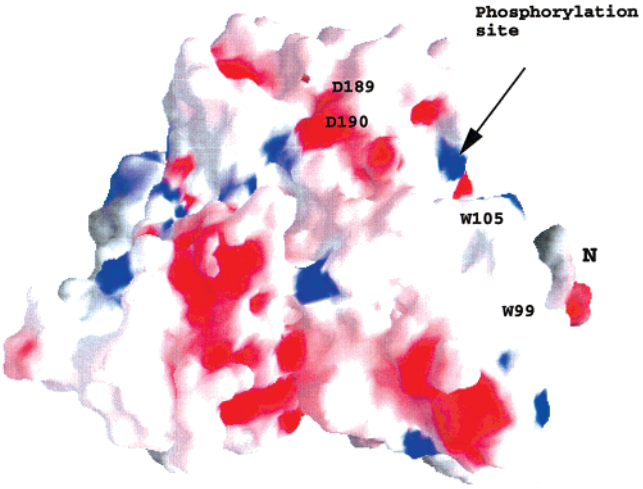

FIGURE 10: Surface of the sorcin calcium-binding domain dimer. The view of the two monomers corresponds to that in Figure 3. In one monomer, the N-terminal residue is indicated by N; the two tryptophan residues (Trp99 and Trp105) on helix D, Asp189 and Asp190 belonging to the charged cluster near the β-sheet structure, and the cAMP-dependent phosphorylation site RRRDS (residues 174−178) are labeled. The picture was generated with GRASP (*30*); the negatively charged residues are red, the positively charged ones blue, and the uncharged ones white.

DISCUSSION

The study presented here provides insight into the structure−function relationships of sorcin as it sheds light on the role played by the N- and C-terminal domains in the two tightly linked Ca^{2+}-dependent processes through which sorcin exerts its biological function, namely, the recognition of target proteins and the Ca^{2+}-induced translocation from cytosol to membranes.

In sorcin, the C-terminal Ca^{2+}-binding domain forms quite stable dimers just like calpain dVI, the prototype of the penta EF-hand family. The soluble SCBD hybridizes in a statistical fashion with the native protein (Figure 4), indicating that the N-terminal domain is not involved in formation of the dimer interface. This finding in addition proves that sequence similarity in the Ca^{2+}-binding domain among the members of the family corresponds to similarity in tertiary and quaternary structure. On this basis, the calpain dVI X-ray coordinates have been used to generate the SCBD model.

The Ca^{2+}-binding sites of the SCBD look very similar to those of the calpain dVI template despite a few differences in the calcium ligands (Figure 1). Thus, the first EF-hand pair, EF1−EF2, is in the open conformation, whereas the second pair, EF3−EF4, and the odd EF5 site are in the closed conformation. In agreement with this picture, the fluorescence titration experiments whose results are reported in Figure 6 and the ultracentrifuge data of Figure 9 show that only two calcium ions bind to sorcin with micromolar affinity and thereby trigger the conformational change that underlies the translocation process. Given the different behavior of the 33−198 and 90−198 fragments, the two physiologically relevant sites can be identified with the EF1−EF2 pair.

It is of interest that the EF1−EF2 pair is involved in the activation of the protein also in calpain dVI. Thus, only this pair is involved in the modest conformational change produced by Ca^{2+} binding which does not lead to detectable changes in the fluorescence properties (*28*). In the SCBD as well, addition of calcium does not alter the intensity of the intrinsic fluorescence (Figure 5B), whereas a significant quenching is observed in the native protein (Figure 5A). These differences, just like the red shift of the fluorescence emission maximum, are accounted for by the SCBD model. In the SCBD, the two tryptophan residues (Trp99 and Trp105), which are both localized in the D helix, are exposed to solvent and form a hydrophobic patch (Figure 10) irrespective of the binding of calcium. In contrast, in the native protein the extent of tryptophan exposure to solvent increases when calcium is bound, a phenomenon that can be ascribed solely to a Ca^{2+}-induced shift of the SCBD relative to the flexible, glycine rich 1−32 N-terminal domain. The hydrophobic patch thereby created on the surface of the SCBD is exploited by sorcin for target protein recognition. In line with this picture, both the SCBD and native sorcin are able to recognize and interact with the ryanodine receptor (Figure 7).

It remains to be established whether sorcin uses the C-terminal domain to interact with all its physiological targets. In annexin VII, Brownawell and Creutz (*8*) mapped the sorcin binding site to the first 31 amino acids in the N-terminal domain, a sequence rich in glycine, proline, and tyrosine residues just like the N-terminal domain of sorcin, and suggested that sorcin may use its N-terminal domain for binding annexin VII. If this suggestion holds true, sorcin may employ different modes of interaction with different target proteins.

In this framework, it is useful to comment on the use of *E. coli* in assessing the membrane-associative properties of sorcin. Interestingly, the topology of interaction delineated by the experiments whose results are reported in Figure 8 closely resembles that pertaining to the ryanodine receptor, thereby validating the use of *E. coli* membranes as a model system.

Last, it is worth mentioning that the proposed Ca^{2+}-linked change in the relative positions of the N- and C-terminal domains may explain the Ca^{2+}-dependent, pH-linked aggregation of sorcin that takes place in the absence of membranes (*4*) and the effect of phosphorylation on the sorcin−ryanodine receptor interaction (*6*). The underlying

assumption is that the charged cluster formed by the EF5 loops near the β-sheet structure, depicted in Figure 10, becomes exposed to solvent upon calcium binding. This cluster comprises Asp171, Asp189, Asp190, and the cAMP-dependent protein kinase recognition site (Arg174, Arg175, Arg176, Asp177, and Ser178) (Figure 1). It may be envisaged that the aspartate residues in this cluster are characterized by abnormally high p*K* values as in polyelectrolytes or small organic molecules such as EDTA (*29*) and hence that they are protonated at pH 6.0 and deprotonated at pH 7.5. These residues therefore could act as calcium ligands only at the higher pH value, consistent with the observation that sorcin undergoes a Ca^{2+}-dependent aggregation at pH 7.5, but not at pH 6.0 (*4*). As far as the protein kinase recognition site RRRDS is concerned, its Ca^{2+}-driven exposure to solvent would facilitate phosphorylation in vitro, consistent with preliminary experiments carried out in this laboratory. In the cell, phosphorylation reduces the ability of sorcin to interact with the ryanodine receptor, a phenomenon which delineates a complex modulation pattern of the Ca^{2+}-linked interaction with the target proteins (*6*).

In conclusion, the study presented here on the structure−function relationship of sorcin demonstrates that the binding site for the ryanodine receptor, the physiological target in muscle cells, maps to the Ca^{2+}-binding domain. It also provides evidence that the novel EF1 motif, which is coupled structurally and functionally to EF2, is endowed with high calcium affinity. In more general terms, the molecular model of the sorcin calcium-binding domain indicates that all members of the penta EF-hand family may share the distinctive features revealed by the calpain dVI prototype structure, namely, the novel mode of calcium coordination, the relatively modest structural rearrangement upon calcium binding, and generation of EF-hand coupling through dimerization. The structures of the whole proteins will elucidate how these new structural motifs are used by the different systems in the interaction with membrane targets to fulfill their specific biological functions.

ACKNOWLEDGMENT

We are grateful to Dr. S. V. L. Narayana for providing the X-ray coordinates of the calpain dVI calcium-binding domain, to Dr. L. Nicolini and Mr. R. Dagai of the Istituto Superiore di Sanità (Rome, Italy) for their invaluable assistance in bacterial growth, and to Drs. G. Mignogna and B. Maras for N-terminal sequence determinations.

REFERENCES

1. Meyers, M. B., and Biedler, J. (1981) *Biochem. Biophys. Res. Commun. 99*, 228−235.
2. Meyers, M. B. (1991) in *Novel Calcium-Binding Proteins. Fundamental and Clinical Implications* (Heizmann, C. W., Ed.) pp 385−399, Springer-Verlag, Berlin, Germany.
3. Meyers, M. B., Zamparelli, C., Verzili, D., Dicker, A. P., Blanck, T. J. J., and Chiancone, E. (1995) *FEBS Lett. 357*, 230−234.
4. Zamparelli, C., Ilari, A., Verzili, D., Vecchini, P., and Chiancone, E. (1997) *FEBS Lett. 409*, 1−6.
5. Meyers, M. B., Pickel, V. M., Sheu, S. S., Sharma, V. K., Scotto, K. W., and Fishman, G. I. (1995) *J. Biol. Chem. 270*, 26411−26418.
6. Lokuta, A. J., Meyers, M. B., Sander, P. R., Fishman, G. I., and Valdivia, H. H. (1997) *J. Biol. Chem. 272*, 25333−25338.
7. Meyers, M. B., Puri, T. S., Chien, A. J., Gao, T., Hsu, P. H., Hosey, M. M., and Fishman, G. I. (1998) *J. Biol. Chem. 273*, 18930−18935.
8. Brownawell, A. M., and Creutz, C. E. (1997) *J. Biol. Chem. 272*, 22182−22190.
9. Chiancone, E., Bull, T. E., Norne, J. E., Forsén, S., and Antonini, E. (1976) *J. Mol. Biol. 107*, 25−34.
10. Van der Bliek, A. M., Meyers, M. B., Biedler, J. L., Hes, E., and Borst, P. (1986) *EMBO J. 5*, 3201−3208.
11. Teahan, C. G., Totty, N. F., and Segal, A. W. (1992) *Biochem. J. 286*, 549−554.
12. Blanchard, H., Grochulski, P., Li, Y., Arthur, J. S. C., Davies, P. L., Elce, J. S., and Cygler, M. (1997) *Nat. Struct. Biol. 4*, 532−538.
13. Lin, G., Chattopadhyay, D., Maki, M., Wang, K. K. W., Carson, M., Jin, L., Youen, P., Takano, E., Hatanaka, M., DeLucas, L. J., and Narayana, S. V. L. (1997) *Nat. Struct. Biol. 4*, 539−546.
14. Maki, M., Narayana, S. V., and Hitomi, K. (1997) *Biochem. J. 328*, 718−720.
15. Kawasaki, H., and Kretsinger, R. (1994) *Protein Profile 1*, 343−349.
16. Greer, J. (1981) *J. Mol. Biol. 153*, 1027−1042.
17. Laskowsky, R. A., MacArthur, M. W., Moss, D. S., and Thornton, J. M. (1993) *J. Appl. Crystallogr. 26*, 283−291.
18. Lüthy, R., Bowie, J. U., and Eisenberg, D. (1992) *Nature 356*, 83−85.
19. Kraulis, J. (1991) *J. Appl. Crystallogr. 24*, 946−950.
20. Edelhoch, H. (1967) *Biochemistry 6*, 1948−1954.
21. Johnson, M., Correia, J. J., Yphantis, D. A., and Halvorson, H. (1981) *Biophys. J. 36*, 575−588.
22. Yang, J. T., Wu, C. S. C., and Martinez, H. M. (1986) *Methods Enzymol. 130*, 208−269.
23. Bryant, D. T. W. (1985) *Biochem. J. 226*, 613−616.
24. Laemmli, U. K. (1970) *Nature 227*, 680−685.
25. Towbin, H., Staehelin, T., and Gordon, J. (1979) *Proc. Natl. Acad. Sci. U.S.A. 76*, 4350−4354.
26. Ikura, M. (1996) *Trends Biochem. Sci. 21*, 14−17.
27. Wyman, J., and Ingalls, E. N. (1943) *J. Biol. Chem. 147*, 297−318.
28. Blanchard, H., Li, Y., Cygler, M., Kay, C. M., Arthur, J. S. C., Davies, P. L., and Elce, J. S. (1996) *Protein Sci. 5*, 535−537.
29. Tanford, C. (1961) *Physical Chemistry of Macromolecules*, pp 548−562, Wiley, New York.
30. Nicholls, A., Bharadwaj, R., and Honig, B. (1993) *Biophys. J. 64*, A166.

BI991648V